ISSN 2621-9883
ELIPSOIDA Vol 4 No 1, September 2021
@Departemen Teknik Geodesi UNDIP

ELIPSOIDA
Jurnal Geodesi dan Geomatika

MODELING OF TSUNAMI RUN-UP USING TERRAIN MODEL DATA BASED ON PHOTOGRAMMETRY PROCESSING PRODUCT

(CASE STUDY AT WAY MULI VILLAGE, RAJABASA, SOUTH LAMPUNG)

Muhammad Ulin Nuha[a,b*], Naufal Hilmi[e], Adhitya Erlangga Pamungkas[e], Chantika Dwi Novita[e], Adam Irwansyah Fauzi[a,b], Aulia Try Atmojo[d], Rizky Ahmad Yudanegara[c]

[a] Research And Innovation Center for Geospatial Information Science, Institut Teknologi Sumatera, Lampung, 35365, Indonesia
[b] Remote Sensing and Photogrammetry Research Group, Geomatics Engineering, Institut Teknologi Sumatera, Lampung, 35365, Indonesia
[c] Geoinformatics and Cadastre Research Group, Geomatics Engineering, Institut Teknologi Sumatera, Lampung, 35365, Indonesia
[d] Geodesy, Surveying, and Hydrography Research Group, Geomatics Engineering, Institut Teknologi Sumatera, Lampung, 35365, Indonesia
[e] Student at Geomatics Engineering, Institut Teknologi Sumatera, Lampung, 35365, Indonesia
*e-mail :muhammad.nuha@gt.itera.ac.id

(Diterima 17 Meil 2021, Disetujui 29 Agustus 2021)

ABSTRAK

Photogrammetry has become a trend in large-scale mapping today. The ability to produce large-scale geospatial products relatively quickly and at low cost is very beneficial for mapping. The power of high temporal and spatial resolution also makes photogrammetry used in the disaster mapping process. In this study, the DEM approach from photogrammetry was used for input data in tsunami run-up modeling activities in Way Muli Village. High temporal and spatial capabilities are utilized to produce surface roughness and elevation, which are critical parameters for rigorous inundation modeling. The modeled inundation results show that the run-up limit achieved in residential areas is on the main road, with a maximum distance of inundation from the shoreline is an average of 80 m. The results obtained can be used by the village government to preparedness in dealing with the tsunami.

Keywords : Run-Up Tsunami, Photogrammetry, Terrain Model, Modelling

ELIPSOIDA
Jurnal Geodesi dan Geomatika

1. Introduction

Disasters are a series of events that threaten people's lives caused by natural factors, non-natural factors, or human factors that result in damage to infrastructure and loss of life (Carter, 2008; Shi, 2019). Indonesia is a country that has vulnerability to the impact of disasters. The country's position is located between 3 (three) active tectonic plates of the world, causing hazards to earthquakes and tsunamis (BNPB, 2016). Located on the ring of fire, Indonesia is prone to volcanic disasters, and its position on the equator makes Indonesia prone to hydrometeorological disasters. (BNPB, 2016).

One of the disaster events that pose a hazard in Indonesia is the tsunami. Tsunami events can be triggered by several factors, such as earthquakes with a high magnitude or the occurrence of underwater landslides. Indonesia recorded 28 tsunami disasters in the 2000 – 2018 (BMKG, 2019). Tsunami disaster management needs attention for the disaster mitigation process to reduce the number of victims and losses. A disaster management process can support tsunami disaster management activities.

Disaster management can begin by identifying the risks posed in an area, followed by identification of vulnerabilities, hazards, and capacities (Coppola, 2015). Disaster management activities can be supported through disaster mapping activities to obtain an overview of the disaster location. Disaster mapping with spatial information about the surrounding area opens up unique geographic trends, and there is a clear spatial-visual pattern that makes it more understandable and helps support the decision-making process (Tomaszewski, 2014). Maps are an essential component used for disaster management (Bandrova et al., 2012).

The mapping process can be used in disaster management activities and one of them is the photogrammetric method. Photogrammetry is a mapping technology that utilizing a camera carried by a flying vehicle (can be a vehicle manned or unmanned) to obtain information on the earth's surface without direct touching objects on the earth's surface (Kasser and Egels, 2002; Kraus, 2007; Everaerts, 2008; Niesen, 2010; Wolf et al., 2014). Photogrammetric technology has high spatial and temporal resolution capabilities. It is suitable for identifying land changes with a high level of detail and current developments by utilizing UAVs to reduce costs in photogrammetric surveys (Everaerts, 2008; Gomez and Purdie, 2016). That capability can be used in the field of disaster management activities.

Photogrammetry in tsunami mapping can be used for the modeling process of tsunami inundation. The product of photogrammetric processing in the form of digital terrain model data can be utilized in the tsunami inundation modeling process (Marfai, et al., 2019). That's because the main data used in the run-up tsunami modeling process are elevation and surface roughness data (Berryman, 2005). The digital terrain model produced by the photogrammetric processing has a very high spatial resolution so that it can produce accurate tsunami run-up model information (Arbad et al., 2019; Marfai, et al., 2019). From the high spatial resolution, the surface roughness will have high detail and resolution of digital terrain models as well.

This research is intended to carry out the tsunami inundation modeling process by utilizing DEM product data from photogrammetric processing. Then a simple modeling process based on a geospatial information system is carried out using the equations developed by Berryman (2005). The modeling results are used to educate the public related to the safe limit of tsunami-affected areas.

2. Materials and Methods

2.1. Research Area

This research focuses on Way Muli Village, Rajabasa District, South Lampung Regency. This location was chosen because of the history of the tsunami that occurred on 22 December 2018. Recording of disaster events is one of the parameters used to disaster risk mapping. The potential for recurrence is one of the backgrounds for researchers to carry out mapping activities in Way Muli Village so that one of the objectives of assessing the tsunami hazard in Way Muli Village is to educate residents about potential tsunami hazard in Way Muli Village. The location of the research focus is shown in the red box presented in **Fig. 1**.

Fig. 1. Research Area

The red box in Fig. 1 is an indicative boundary used to take on the acquisition process of aerial photo mapping in Way Muli Village then adjusted to field conditions.

2.2. Photogrammetry Concept

Photogrammetry is a mapping technology by utilizing a camera carried by a flying vehicle (can be a vehicle manned or unmanned) to obtain information on the earth's surface without direct touching objects on the earth's surface (Kasser and Egels, 2002; Kraus, 2007; Everaerts, 2008; Niesen, 2010; ;Wolf et al., 2014). In aerial photography geometry, an aerial photograph can obtain three-dimensional information by utilizing the nature of human vision. This uses the way the human brain works every time it gets two images that slightly differ because each position of the left eye and right eye perceives according to the eye's central point of view or overlap (Linder, 2006). This principle in photogrammetry is known as the stereoscopic principle (Linder, 2006; Kraus, 2007; Wolf et al., 2014). The stereoscopic geometry is shown in **Fig. 2**.

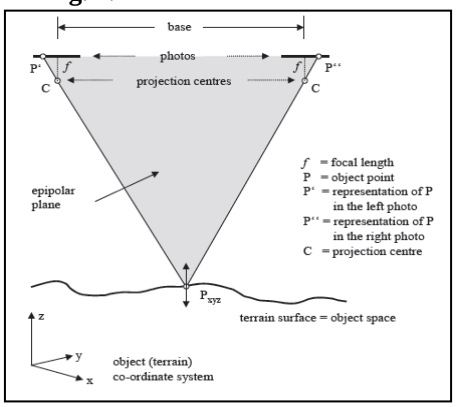

Fig. 2. Stereoscopic Geometry ((Linder, 2006)

Stereoscopic to obtain three-dimensional information in photogrammetry by having two photos overlapping each other so that the three-dimensional coordinates of each point that are the same in the two photos can be calculated. In photogrammetric mapping, there are important principles for photogrammetric processing. This principle is the principle of orientation to obtain information on the earth's surface objects in three-dimensional ground coordinates. Orientation in aerial photography consists of interior orientation, exterior orientation, absolute orientation, and relative orientation (Linder, 2006).

2.3. Flight Planning

The work before starting the acquisition of aerial photo data is flight planning. This is intended for aerial photography work that can record 3D objects on the earth's surface (Kraus, 2007). In this study, a DJI Phantom 4 Advanced quadcopter was used which carried a camera sensor with the parameters shown in **Table 1** for this project.

Table 1. Camera Parameter

Parameter	Value
Focal length	8.8 mm
Solid State	1-Inch 20-megapixel CMOS sensor (4864 x 3648)
Pixel Size	2,6 mikron

Camera parameters are used to calculate ground sampling distances (GSD). GSD is the smallest size of the object that can be recorded by the aerial photo which can be calculated using a function of flying height, focal length, and pixel size (Wolf et al., 2014). The calculation of GSD is shown by the following formula.

$$\frac{pixel\ size}{GSD} = \frac{focal\ length}{flying\ height} \quad \textbf{(1)}$$

Usually the camera parameters are known and the GSD is required so that calculations are carried out to calculate the value of the flying height of the vehicle.

2.3. DEM Generation

Digital Elevation Model is a representation of the bare earth surface (without containing surface information like a tree, building, and etc.). DEM can be produced using many methods like topographic mapping, LiDAR Mapping, Satellite Photogrammetry, and Photogrammetric Mapping (Aerial). The method of producing DEM has advantages and disadvantages such as time, complexity, and cost. Photogrammetry can produce

DEM in a short time and low cost, but the complexity of processing becomes a challenge in the production of DEM (Uysal et al., 2015). In photogrammetry, DEM is produced using the stereo concept (Linder, 2006). DEM is obtained from overlapping photos in a stereo model which results in a 3D object with a height value (ilustrated by **Fig. 3**).

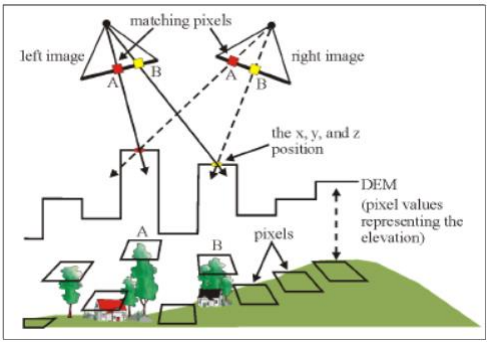

Fig. 3. DEM Generation by Photogrammetry (Source : Manual Guide PCI 9.1)

The original photogrammetry product is a Digital Surface Model (DSM) because aerial photography records the entire object under the camera sensor. DSM can be produced with stereoscopic or computer vision using structure from motion (Linder, 2006; Fleury et al., 2016). To obtain terrain or bare earth surface information, the image matching point cloud data must be filtered to remove the surface objects (Uysal et al., 2015).

2.4. Ortho Generation

Orthophoto is a product of photogrammetric processing whose quality depends on the accuracy of the camera pamarameter, the camera calibration process, and photo orientation along with digital elevation data and the quality of the ground control points used in the process (Kraus, 2007; Barazzetti, et al., 2014). Ortho Generation uses DSM in the process to remove the relief displacement that occurs in photos and when using additional digital building information (obtained from LiDAR processing) it can produce true orthophotos (Jarvis, 2008; Wolf et al., 2014).

True orthophoto production evade the double-mapping problem by performing a visibility analysis procedure to identify enclosed areas in object space. The resulting true orthophoto quality is controlled by the quality of the georeferenced parameters of the surface model from LiDAR. However, the irregular nature of the LiDAR data leads to degraded quality of the building boundaries on the DSM interpolation. This degradation in DSM quality can cause a scissoring effect on building boundaries when the resulting true orthophoto (Habib, et al, 2008)**.**

2.5. Accuracy on Photogrammetric Product

Assessment of the quality of photogrammetric product data uses the provisions of the Regulation of the Head of the Geospatial Information Agency Number 1, 2020 about Standards for Geospatial Data Collecting for Large-Scale Mapping and SNI 8202 – 2019 about Base Map Accuracy. The product results must be better than 0.5 from the accuracy of the base map that refers to SNI 8202 – 2019.

2.6. Tsunami Modelling Based on GIS

A tsunami is a series of high-speed moving waves triggered by an earthquake, an erupting sea volcano, or an underwater landslide (Berryman, 2005). The tsunami hazard parameter is the potential for inundation (inundation) on land based on the potential maximum wave height that arrives at the coastline. The spatial distribution of the area affected by the tsunami inundation can be made from the results of mathematical calculations developed by Berryman (2005) based on the calculation of tsunami height loss per 1 m of inundation distance (inundation height) based on the distance to the slope and surface roughness. The calculation of inundation model is shown by the following formula.

$$H_{loss} = \left(\frac{167n^2}{H_0^{\frac{1}{3}}} \right) + 5 \sin S \qquad \textbf{(2)}$$

Where H_{loss} is the loss of tsunami height per 1 m of inundation distance, n is the coefficient of surface roughness obtained from orthophoto information (, H_0 is the height of tsunami waves on the shoreline in meters determined based on the recording incident history, and S is the degree of a surface slope calculated from photogrammetric DEM. The classification of surface roughness is obtained from Berryman (2005).

3. Results and Discussion

3.1. Aerial Triangulation

This study used six Ground Control Points (GCPs) and four independent Check Points (ICPs) for the aerial triangulation process. All ground control points and checks are spread along the shoreline due to the shape of the area that extends along the shoreline. Based on photogrammetry, the control point used is not ideal because it only focuses on locations near the coast so that the quality of the highlands in the Way

Muli area is not recorded. The following **Fig. 4** shows the distribution of control points.

Fig. 4. Distribution of GCPs and ICPs

The horizontal coordinates use the UTM projection system in the 48S zone and the vertical coordinates use the geoid system which is processed through the srgi.big.go.id. Photogrammetric processing is carried out using software based on Structure from Motion. The processing results obtained that the precision of the coordinates of GCPs in 3D is at a value of 4.52 cm with a pixel error of 1.2 pixels and the accuracy of the coordinates of ICPs in 3D is at a value of 36.23 cm with a pixel error of 0.5 pixels (presented in **Table 2**).

Table. 2. Triangulation Report

Component	RMSE			Error Pixel (Pix)
	Hz. (cm)	Vz. (cm)	3D (cm)	
Accuracy/GCPs	4.51	0.22	4.52	1.2
Precision/ICPs	21.90	28.86	36.23	0.5

The results of aerial triangulation were tested based on map accuracy standards in Indonesia. For aerial triangulation results, the ICPs test must be better than 0.4 of the base map accuracy required by SNI 8202 – 2019. CE90 and LE90 are 0.33 and 0.48. If referring to the prerequisites, the CE90 and LE90 (must be better 0.4 than the accuracy of the base map in SNI 8202-2019) are 0.83 and 1.19. Then the aerial triangulation results pass for the 1:2500 Class 1 scale map for horizontal accuracy with contour intervals of 2 m.

3.2. Ortho Generation

The flight mission was taken on at an average altitude of 150 m above sea level with a total of 731 images obtained from aerial photographs. The standard overlap and sidelap used is 75% (needs for non-metric photogrammetric mapping which requires high overlap and sidelap). The results of photogrammetry processing get a spatial resolution value of 3.89 cm/pix with a reprojection error of 0.384 pix. Orthophoto results are shown in **Fig. 5**.

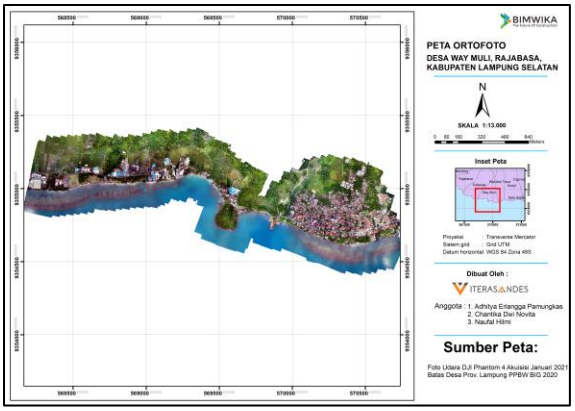

Fig. 5. Orthophoto Result

Orthofoto quality control results include two things: refers to the value of GSD and RSME value. GSD is the pixel size of the object being photographed, the smaller the GSD, the better the accuracy of the object being photographed. While RMSE is the geometry correction accuracy of a photo, the smaller the RMSE, the accuracy of the object resulting from the shooting will be better too.

Furthermore, the orthophoto results were tested for horizontal accuracy by extracting the ICP values obtained from the orthophoto and ICP results from field measurements. The horizontal RMSE value obtained is 0.092 m with the CE90 calculation result is 0.140 m. If it refers to the applicable standard, the orthophoto result must be in the accuracy range better than 0.5 of the map standard accuracy value according to SNI 8202 – 2019. This means that the final orthophoto product pass for the 1:1000 class 1 scale map for horizontal accuracy.

3.3. Digital Terrain Model Generation

Products elevation models produced there are two of DSM and DTM. DSM is the first product obtained from photogrammetric processing. The resulting DSM has a minimum height of -5.65m and a maximum height of about 94 meters. **Fig. 6** shows the results of the DSM.

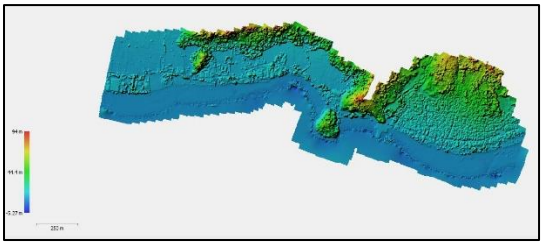

Fig. 6. DSM Result

Furthermore, the results of the DSM filtering process using the slope-based filtering (SBF) method on the SfM-based photogrammetric processing application. The results obtained are the minimum height of the DTM is -5.65m and the maximum height is 80.7m. There is not much difference because the filtering process is carried out semi-automatically on the basis that only the coastal area is important to obtain accurate DTM data. **Fig. 7** shows the results of DTM.

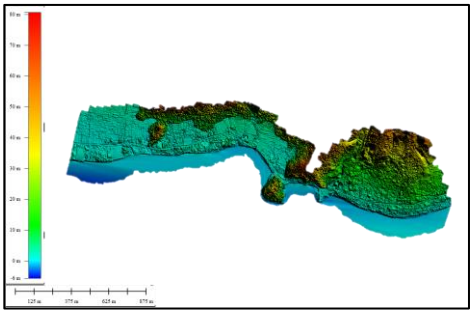

Fig. 7. DTM Result

Then, the DEM data is tested at vertical accuracy according to the applicable reference. Using the measured ICPs and the same procedure when testing orthophoto results. The result of the vertical RMSE calculation is 0.127m. LE90 calculation process is carried out which produces a value of 0.209. In accordance with the applicable regulations, using a reference must be better than 0.5 of the map accuracy value in SNI 8202 – 2019. The calculated results show the results of the entry elevation model at a contour interval of 0.4m in class 2.

3.4. Tsunami Modelling

The tsunami modeling is done by using the model developed by Berryman (2005). Orthophoto results are used to derive surface roughness information through land cover. DEM results are used as elevation in the run-up model. The DEM used was taken at a spatial resolution of 8 cm and Orthophoto was used at a spatial resolution of 3.89 cm. The following modeling results is shown in **Fig. 8**.

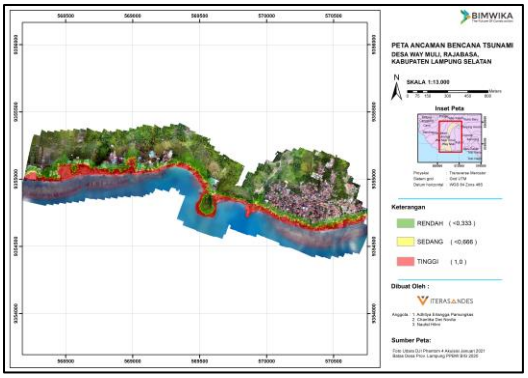

Fig. 8. Inundated Area for Tsunami Modeling

Results of the tsunami inundation model then recount coverage of the area affected by the tsunami inundation model. Of calculating the areas affected by inundation, Village Way Muli is an area prone to high levels of vulnerability class that area were flooded area of 9.7 hectares with a total area of 21.3 hectares affected. The total area of the affected area is presented in **Table 3**.

Table. 3. the extent of the affected area

Inundation Level	Affected Area (ha)
< 1 m	**8,903**
1 - 3 m	**2,682**
> 3 m	**9,713**
Total	**21,298**

Due to the high level of tsunami hazard, this will also have an impact on economic losses that will be experienced by the residents of Way Muli Village, there are 786 houses affected by the tsunami from this model. In addition, the majority of the livelihoods of local residents are farmers, fishermen, and fish farming, this will be very detrimental to the residents if a tsunami occurs. Therefore, this threat level map can help the government and local villagers in anticipating the effect of a tsunami hazard.

3.5. Mitigation and Preparedness

Results of research conducted can be used for mitigation processes both structural and non-structural. Structural mitigation can be done by making warning signs and self-rescue in Way Muli Village by the Government. In this phase of the national or the provincial government, such as the construction of breakwaters can be done to reduce the rate of propagation of the tsunami wave energy.

The model results showed that the maximum limit of tsunami inundation on the main road. The model calculated the approximate height of the tsunami to

10m. The village government is recommended to provide education for people's understanding regarding the potential catastrophic tsunami and the potential for recurrence. The average distance of 80 meters is the maximum coverage area that can be reached by the propagation of tsunami waves.

The maximum range that occurs is also supported by the condition of the Way Muli landforms ranging from mountain and coastal landscapes. Distance from the beach is 80 meters and the contours of the village began to rise in the distance (area after the main road away from the beach). The condition can be used as a potential area for the rescue of the tsunami disaster in the village of Way Muli.

4. Conclusion

From the results and discussion can be drawn a conclusion that a tsunami model obtained from the modeling done can be a picture of the area that survived the tsunami hazard in the village of Way Muli. The impact that may occur is about 786 houses exposed to the impact of the tsunami inundation. The modeled inundation results show that the run-up limit achieved in residential areas is on the main road with a maximum distance of inundation from the shoreline is an average of 80 m. The results obtained can be used by the village government to preparedness in dealing with the tsunami.

Suggestions for this research are the addition of capacity and vulnerability information that can be used to calculate the tsunami risk index in Way Muli Village. The results of the risk may be used to calculate the value of losses that may arise as a result of the tsunami in the village of Way Muli. And also the photogrammetric accuracy can be enhanced by the placement of the design process of the best control points according to the rules of photogrammetry to minimize the appearance of the bowl effect on the results.

Acknowledgements

The authors are grateful to the Way Muli village government and the way muli village community fully support the mapping activity at Way Muli Village. From these activities, authors' research can run well and can produce research works for lecturers and students. Furthermore, we also truly thankful for administrative support from the Research And Innovation Center of Geospatial Information Sciences, Institut Teknologi Sumatera. And thank you to our beloved team, ITERASANDES, who have struggled and worked together in this research work.

References

Arbad, A. P., Takeuchi, W., Jonathan, S., Jamilah, M., Ardy, A., & Meimuna, C. (2019). Western lampung probabilistic tsunami hazard model: investigations by aerial photogrammetry and remote sensing data. *The 40th Asian Conference on Remote Sensing*. Daejeon, Korea.

Bandrova, T., Zlatanova, S., & Konecny, M. (2012). Three-dimensional maps for disaster management. *ISPRS - International Archives of the Photogrammetry, Remote Sensing and Spatial Information Sciences*, (July). https://doi.org/10.5194/isprsannals-I-4-245-2012

Barazzetti, L., Brumana, R., Oreni, D., Previtali, M., & Roncoroni, F. (2014). True-Orthophoto Generation From Uav Images : Implementation Of A Combined Photogrammetric And Computer Vision Approach. *ISPRS Annals of the Photogrammetry, Remote Sensing and Spatial Information Sciences*, *II*(June), 23–25. https://doi.org/10.5194/isprsannals-II-5-57-2014

Berryman, K. (2005). *Review of Tsunami Hazard and Risk in New Zealand*. New Zealand: Institute of Geological & Nuclear Sciences.

BMKG. (2019). *Katalog Tsunami Indonesia Tahun 416-2018*. Jakarta Pusat, DKI Jakarta: Pusat Gempabumi dan Tsunami, Kedeputian Bidang Geofisika, BMKG.

BNPB. (2016). *Risiko Bencana Indonesia*. Badan Nasional Penanggulangan Bencana Indonesia.

Carter, W. N. (2008). *Disaster Management*. Manila, Philippines: Asian Development Bank.

Coppola, D. P. (2015). *Introduction to International Disaster Management* (3rd ed.). Oxford, UK: Butterworth-Heinemann.

Everaerts, J. (2008). The use of unmanned aerial vehicles (uavs) for remote sensing and mapping. *The International Archives of the Photogrammetry, Remote Sensing and Spatial Information Sciences*, *XXXVII*(Part B1), 1187–1192.

Fleury, J. T., Brunier, G., Fleury, J., Anthony, E. J., Gardel, A., & Dussouillez, P. (2016). Structure-from-Motion photogrammetry for high-resolution coastal and fluvial geomorphic surveys Geomorphology Close-range airborne Structure-from-Motion Photogrammetry for high-resolution beach morphometric surveys : Examples from an embayed rotating beach. *Geomorphology*, *261*(May), 76–88. https://doi.org/10.1016/j.geomorph.2016.02.025

Gomez, C., & Purdie, H. (2016). UAV- based

Photogrammetry and Geocomputing for Hazards and Disaster Risk Monitoring – A Review. *Geoenvironmental Disasters*. https://doi.org/10.1186/s40677-016-0060-y

Habib, A. F., Kersting, J., McCaffrey, T. M., & Jarvis, A. M. Y. (2008). Integration of lidar and airborne imagery for realistic visualization of 3D urban environments. *Proceedings of the International Society for Photogrammetry, Remote Sensing and Spatial Information Sciences,(ISPRS Congress)*, 617–623.

Jarvis, A. M. Y. (2008). Integration of Photogrammetric and LIDAR Data for Accurate Reconstruction And Visualization of Urban Environments. University of Calgary.

Kasser, M., & Egels, Y. (2002). *Digital Photogrammetry*. London: Taylor & Francis.

Kraus, K. (2007). *Photogrammetry* (2nd ed.). Vienna: de Gruyter Textbook.

Linder, W. (2006). *Digital photogrammetry* (3rd ed.). Jerman: Springer.

Marfai, M. A., Fatchurohman, H., & Cahyadi, A. (2019). An Evaluation of Tsunami Hazard Modeling in Gunungkidul Coastal Area using UAV Photogrammetry and GIS . Case Study : Drini Coastal Area. *ICENIS*, *5*.

Niesen, M. (2010). Introduction to Small-Format Aerial Photography. *Nineteenth Century*, (September 2008), 1–13. https://doi.org/10.1016/B978-0-444-53260-2.10001-8

Shi, P. (2019). *Disaster Risk Science*. China: Springer.

Tomaszewski, B. (2014). *Geographic Information Systems (GIS) for Disaster Management*. Boca Raton: CRC Press.

Uysal, M., Toprak, A. S., & Polat, N. (2015). Dem generation with uav photogrammetry and accuracy analysis in sahitler hill. *MEASUREMENT*, (June). https://doi.org/10.1016/j.measurement.2015.06.010

Wolf, P., DeWitt, B., Wilkinson, B., & Wolf. (2014). *Elements of Photogrammetry with Application in GIS* (4th ed.). New York: McGraw-Hill Education.